

## pH Dependence of the Reversible and Irreversible Thermal Denaturation of $\gamma$ Interferons<sup>†</sup>

Michael G. Mulkerrin\* and Ronald Wetzel

Department of Biomolecular Chemistry, Genentech Inc., 460 Point San Bruno Boulevard,  
South San Francisco, California 94080

Received December 30, 1988; Revised Manuscript Received May 3, 1989

**ABSTRACT:** Heated at pH 6.0 and at 50 °C, human interferon  $\gamma$  (HuIFN- $\gamma$ ) is inactivated via the formation of insoluble aggregates. At pH 6.0, the aggregation rate increases with temperature from 40 to 65 °C. There is a temperature-dependent time lag to aggregate formation observed in the generation of light-scattering particles at pH 6.0, and this correlates with the fast phase observed in the kinetics of reversible thermal unfolding. In addition, the dependence of aggregation kinetics on temperature closely follows the reversible melting curve. These observations suggest that at pH 6.0 irreversible thermal denaturation and aggregation depend on partial or complete unfolding of the molecule. At pH 5.0, also at 50 °C, the molecule is stable to irreversible aggregation. In reversible unfolding in 0.25 M guanidine hydrochloride, the  $T_m$  for HuIFN- $\gamma$  increases from 30.5 °C at pH 4.75 to 41.8 °C at pH 6.25, in analogy to the behavior of other globular proteins. These observations suggest that the relative instability of HuIFN- $\gamma$  to irreversible denaturation via aggregation at pH 6.0 compared to pH 5.0 is not due to an increased stability toward unfolding at the lower pH. Alternatively, stability at pH 5.0 must be due either to the improved solution properties of the unfolded state or to the improved solubility/decreased kinetic lifetime of an unfolding intermediate. Aggregation of HuIFN- $\gamma$  at 50 °C is half-maximal at pH 5.7, suggesting that protonation of one or both of the histidine residues may be involved in this stabilization. This hypothesis is supported by chemical modification experiments in which reaction with the histidine-specific reagent ruthenium pentaamine eliminates aggregation of the thermally unfolded molecule at pH 6.0. Histidine involvement may also explain our finding that rabbit interferon  $\gamma$  and bovine interferon  $\gamma$  do not aggregate in the pH range of 5.0–6.0 at temperatures close to their  $T_m$ s.

Interferon  $\gamma$  is a 17 000-dalton molecule that forms a dimer of identical subunits exhibiting antiviral, antiproliferative, and immunoregulatory properties on a variety of mammalian cells (Langer & Pestka, 1985). Algorithms for secondary structure prediction suggest the molecule to be high in  $\alpha$  helix (Zoon & Wetzel, 1984), and this is supported by circular dichroism studies (Arakawa et al., 1985). Human interferon  $\gamma$  (HuIFN- $\gamma$ )<sup>1</sup> contains no disulfide bonds, and the  $pI$  is calculated to be 10.0 from the amino acid content. Although the natural material does contain N-linked carbohydrate (Rinderknecht et al., 1984), the nonglycosylated protein produced by expression of the cloned gene in *Escherichia coli* has essentially the same specific activity as natural material (Gray et al., 1982). IFN- $\gamma$  is distinguished from other members of the interferon family by the inability to recover activity after exposure to low pH, and the nature of the sensitivity of *E. coli* produced HuIFN- $\gamma$  to pH 2 treatment has been well characterized (Arakawa et al., 1985). In contrast, the pH dependence of the structure and solution properties of the molecule in the neutral pH range has not been explored in detail.

To assess the effects of amino acid substitutions on the thermodynamic stability of HuIFN- $\gamma$ , we have begun the characterization of the stability of wild-type HuIFN- $\gamma$  produced in *E. coli*. As is the case for many globular proteins, these studies were initially encumbered by the irreversibility of thermal unfolding at neutral pH due to or accompanied by aggregation. In the course of defining a system allowing

reversible thermal unfolding, we initiated a detailed characterization of the relationship between reversible unfolding and irreversible denaturation of this molecule, and the ways in which changes in the pH range 4–8 affect these processes.

Thermal irreversible denaturation of proteins, by physical effects such as aggregation, precipitation, and adsorption, is generally viewed as being mediated by unfolding to produce a statistical coil conformation with poor solution properties (Lumry & Eyring, 1960; Lumry & Biltonen, 1968). Both the electrostatic nature and the hydrophobic nature of the newly exposed residues determine, as an ensemble, the solubility of the unfolded polypeptide. Thermal aggregation thus is considered a global phenomenon of the statistical coil and not strongly dependent on a specific residue.

Changes in pH might be expected to influence the thermal inactivation process in a number of ways, for instance, by altering the conformational free energy of the folded polypeptide and/or by altering the solubility properties of the folded or unfolded protein. Any of these pH effects would, in general, be expected to operate via a broad pH dependence, consistent with the importance of the global electrostatic free energy contribution to these processes (Matthew, 1985; Matthew et al., 1985).

<sup>1</sup> Abbreviations: interferon  $\gamma$ , IFN- $\gamma$ ; human interferon  $\gamma$ , HuIFN- $\gamma$ ; bovine interferon  $\gamma$ , BoIFN- $\gamma$ ; HPLC, high-pressure liquid chromatography; TFA, trifluoroacetic acid;  $T_m$ , temperature of half-maximal unfolding. The sequence numbering convention is that described by Wetzel (1988), where residue 1 is the first residue of the mature protein as expressed in mammalian tissue. Material used in this study is produced in *Escherichia coli*; therefore, the additional N-terminal methionine is residue -1.

<sup>†</sup> This work was presented in part at a meeting of the International Society for Interferon Research (Mulkerrin & Wetzel, 1987).

\* Correspondence should be addressed to this author.

In this paper, we show that the irreversible thermal denaturation of HuIFN- $\gamma$  is correlated with thermal unfolding, consistent with the classical mechanism. We also show that the pH dependence of thermal irreversible denaturation is determined by the effect of pH on the solution properties of an unfolded state of the protein, not by the effect of pH on the stability of the folded protein. This pH dependence occurs over a narrow range, between pH 5.0 and pH 6.0. Several lines of evidence suggest that the thermally unfolded molecule aggregates readily when one or both of its two histidine residues are deprotonated.

## EXPERIMENTAL PROCEDURES

**Materials.** Recombinant DNA derived HuIFN- $\gamma$ , BoIFN- $\gamma$ , and rabbit IFN- $\gamma$  are purified from *Escherichia coli* extracts. HuIFN- $\gamma$  used here possesses the initial methionine at position -1 and ends with the C-terminal arginine at position 139 of the natural sequence. The activity is determined in the cytopathic effect inhibition microtiter assay (Rubinstein et al., 1981).

Protein concentrations are determined by using an  $\epsilon^{0.1\%}$  of 0.75 at 280 nm for HuIFN- $\gamma$ , BoIFN- $\gamma$ , and rabbit IFN- $\gamma$ .

**Aggregation Assay.** Aggregation is monitored as the increase in optical density, turbidity, at 340 nm in a Kontron Uvikon 810 UV-visible spectrophotometer. The relationship between optical density (OD) and turbidity ( $\sigma$ ) is given by (Leach & Scheraga, 1960)

$$\log(I/I_0) = OD = e^{-\sigma x} \quad (1)$$

Turbidity, in turn, is related to the concentration ( $c$ ) and the molecular weight ( $M$ ) of the light-scattering particles according to eq 2.  $H$  is an optical constant for any sample

$$\sigma = HcM \quad (2)$$

of constant particle size and concentration (Cancellieri et al., 1974).

Equations 1 and 2 show that optical density increases as a function of the increase in molecular weight and concentration of the light-scattering particles. In the spectral region where a protein does not absorb incident radiation, turbidity can be used to determine the particle size. The major caveat is the aggregate must be monodisperse in order to determine the aggregate molecular size. Over the time course of the experiments described here, as interferon aggregates, there is a continual increase in both the size and concentration of the aggregated protein. Consequently, we are monitoring an increase in turbidity as a measure of the total mass of aggregated protein irrespective of the concentration and size of the aggregate. Therefore, we report the aggregation in relative terms as OD and the rate of aggregation as  $\Delta OD/\text{min}$ .

**Preparation of Samples for Aggregation Analysis.** Samples of IFN- $\gamma$  are equilibrated with 0.01 M acetic acid, pH 5.0, and concentrated by using a Centricon 10 microconcentrator (Amicon). The buffer used in the determination of the pH dependence of aggregation of HuIFN- $\gamma$  is 0.05 M in acetic acid with Tris base added to bring the solution to the indicated pH. In reactions performed at pH 5.0, the buffer is 0.01 M acetic acid, and reactions at pH 6.0 are performed with 0.01 M sodium succinate titrated with HCl. Before the aggregation reaction is initiated, the buffer is equilibrated in the cuvette at the temperature indicated in the figure legends. For the aggregation reactions, HuIFN- $\gamma$ , BoIFN- $\gamma$ , or rabbit IFN- $\gamma$  is added to the buffer solution. The reaction is initiated when protein is added to bring the total protein to 0.1 OD at 280 nm in a total volume of 1.0 mL, or 75  $\mu\text{g/mL}$ .

**HPLC of HuIFN- $\gamma$ ,  $\text{Ru}^{3+}(\text{NH}_3)_5\text{-HuIFN-}\gamma$ , and Ethoxyformyl-HuIFN- $\gamma$ .** HPLC was performed by using a Waters Model 720 controller and two Waters Model 510 pumps. The detector is a Waters Model 490 detector with the output directed to a Kipp and Zonen two-pen chart recorder. Both 214 nm and 280 nm are recorded for the resolution of proteins except for the ruthenium pentaammine labeled HuIFN- $\gamma$  where 214 nm and 320 nm are monitored. The solvents used in the HPLC are the following: solvent A, water 0.1% in TFA; solvent B, acetonitrile 0.1% in TFA.

**Preparation of Pentaammineruthenium(III)-HuIFN- $\gamma$ .**  $\text{Ru}^{3+}(\text{NH}_3)_5\text{Cl}$  (AESAR, Seabrook, NH) (0.005 mol) is dissolved into 250  $\mu\text{L}$  of 0.01 M acetic acid, pH 5.0. Once this has dissolved, the solution is centrifuged, and 200  $\mu\text{L}$  of the supernatant is added to 8.9 mg of HuIFN- $\gamma$  in 0.5 mL. This is allowed to react until all of the HuIFN- $\gamma$  is labeled, as indicated by HPLC analysis.

**Circular Dichroism Instrumentation.** Thermal denaturation profiles are obtained by using an automated Jasco J-500 spectropolarimeter as described previously (Mulkerrin et al., 1986). The spectropolarimeter is calibrated with *d*-10-camphorsulfonic acid (Chang & Yang, 1977). The algorithm used for the collection of the thermal denaturation profiles as well as the details of the instrumentation is to be published elsewhere (Mulkerrin, unpublished results).

**Thermal Denaturation of HuIFN- $\gamma$ .** In order to acquire reversible thermal denaturation profiles above pH 5.0, it is necessary to include 0.25 M guanidine hydrochloride (Research Plus, Bayonne, NJ), which is sufficient to prevent aggregation and allow reversible unfolding. Guanidine hydrochloride at 0.25 M is below the concentration necessary to begin to unfold the molecule at room temperature, though it does reduce the  $T_m$  of the molecule. Tanford (1964) has shown that the change in the free energy of the native to unfolded transition of a macromolecule is a linear function of the interaction of the macromolecule with a denaturant. Therefore, at pH 6.0, thermal denaturation profiles were obtained by using decreasing concentrations of guanidine hydrochloride, the  $T_m$  values obtained are plotted, and a linear extrapolation to 0.0 M guanidine hydrochloride yielded the corrected  $T_m$ .

## RESULTS

The aggregation of HuIFN- $\gamma$  shown in Figure 1 is a plot of the  $OD_{340}$  vs time of identical concentrations of HuIFN- $\gamma$  heated at various temperatures. Although aggregation at 40  $^\circ\text{C}$  is not measurable by  $OD_{340}$  (Figure 1), precipitated protein is evident in the cuvette after overnight incubation. At the conclusion of an assay in the 50–60  $^\circ\text{C}$  range (when the  $OD_{340}$  is no longer changing), less than 10% of the HuIFN- $\gamma$  remains in solution. An interesting feature of the aggregation kinetics in Figure 1 is the observed decrease in the lag time before the onset of aggregation as the temperature increases. As, discussed below, our data suggest, this is related to the population of unfolded molecules accumulating more slowly at lower temperatures.

The thermal unfolding of HuIFN- $\gamma$  is reversible at pH 5.0. Hence, the unfolding kinetics, measured by ellipticity changes at 222 nm, can be determined at pH 5.0 without interference from aggregation. In these unfolding experiments, two processes are observed (Mulkerrin, unpublished results). A double-exponential decay of the ellipticity suggests there are two unfolding events. The fast phase is variable and dependent on temperature while the slower is independent of the temperature with a half-time for unfolding of just over an hour. The aggregation lag times at pH 6.0 and the kinetic half-times for the fast phase of the unfolding at various temperatures are

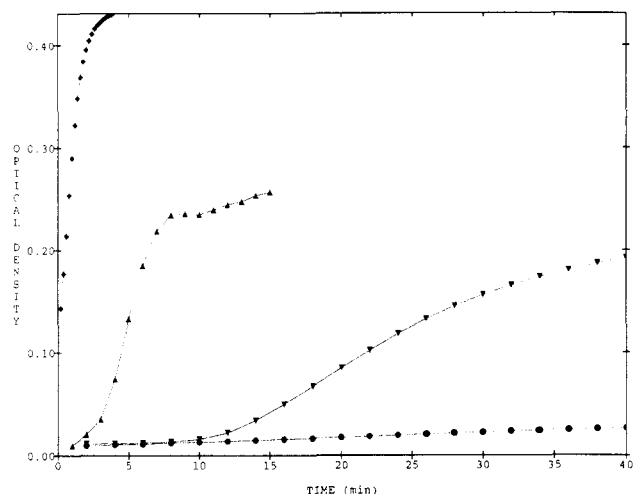


FIGURE 1: Change in optical density at 340 nm versus time. Optical density at 340 nm is used as a measure of aggregation. Samples contain 7  $\mu$ L of HuIFN- $\gamma$  at 19.05 mg/mL added to 993  $\mu$ L of 0.01 M succinate buffer, pH 6.0. Aggregation is measured at increasing temperatures: 45  $^{\circ}$ C ( $\bullet$ ); 50  $^{\circ}$ C ( $\nabla$ ); 55  $^{\circ}$ C ( $\Delta$ ); and 60  $^{\circ}$ C ( $\blacklozenge$ ).

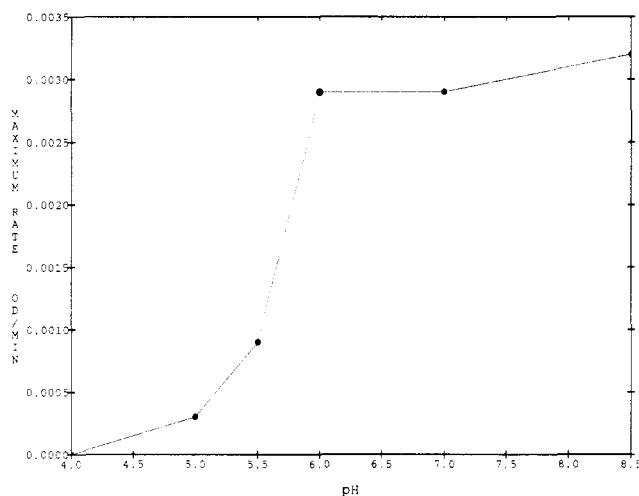


FIGURE 2: Aggregation versus pH. Buffers are 0.05 M acetic acid and titrated to the indicated pH with Tris base. Each assay is 0.10 OD<sub>280</sub> in HuIFN- $\gamma$  (75  $\mu$ g/mL). The maximum rate in  $\Delta$ OD/min is plotted versus pH. Samples were heated at 50  $^{\circ}$ C.

Table I: Thermal Unfolding of HuIFN- $\gamma$

temp ( $^{\circ}$ C)	aggregation lag time (min) at pH 6.0	unfolding $t_{1/2}$ (min) <sup>a</sup> at pH 5.0
45	ND	33.9
50	10	8.8
55	1	4
60	<1	1.2

<sup>a</sup> For the fast phase of unfolding. See text.

presented in Table I. The lag times in the 50 and 55  $^{\circ}$ C aggregation reactions at pH 6.0 are of the same order of magnitude as the half-lives of the fast phase of unfolding at these temperatures. At 40  $^{\circ}$ C, the aggregation is quite slow and is not detectable in the aggregation assay. On this time scale, the particles do not achieve sufficient size at a high enough concentration to increase the optical density. At 60  $^{\circ}$ C, the aggregation is fast, and no lag time is seen with these techniques, consistent with the fast unfolding rate at this temperature.

Figure 2 shows the pH dependence of the aggregation at 50  $^{\circ}$ C. Below pH 4.5, the molecule is known to spontaneously unfold to give a soluble aggregate (Yphantis & Arakawa,

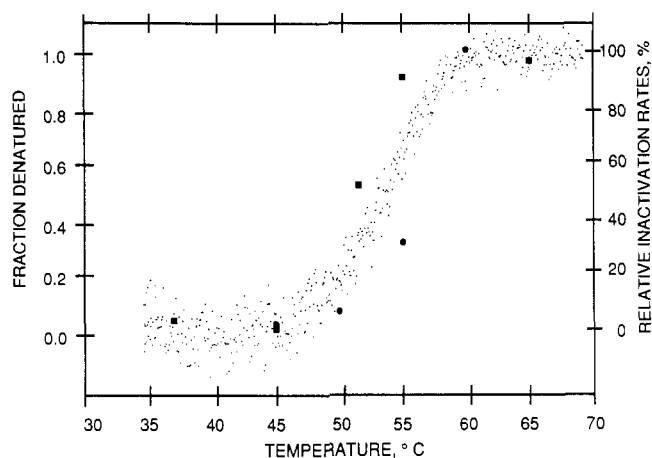


FIGURE 3: Thermal denaturation of HuIFN- $\gamma$  and aggregation versus temperature. The thermal denaturation profile (small circles) is determined in 0.25 M guanidine hydrochloride/0.01 M succinate, pH 6.0, and corrected to 0.0 M guanidine hydrochloride. The aggregation ( $\bullet$ ) is the relative maximum  $\Delta$ OD/min taken from Figure 2. The filled squares indicate the mole fraction of HuIFN- $\gamma$  still accessible to a monoclonal antibody after being heated for 90 min. Identical samples of 0.25  $\mu$ g/mL HuIFN- $\gamma$  in phosphate-buffered saline containing 0.5% bovine serum albumin are heated at the indicated temperatures, cooled, and then assayed by ELISA (Foon et al., 1985).

Table II: Thermal Denaturation of HuIFN- $\gamma$ <sup>a</sup>

pH	$T_m$ ( $^{\circ}$ C)	pH	$T_m$ ( $^{\circ}$ C)
4.75	30.5	5.75	42.5
5.00	35.5	6.00	41.0
5.22	38.4	6.25	41.8
5.50	40.5		

<sup>a</sup> Samples include 0.25 M guanidine hydrochloride.

1987). At pH 5.0, the molecule reversibly unfolds when heated. Upon cooling, approximately 80% of the ellipticity at 222 nm is recovered within the first 2 h. After the sample is allowed to refold for several days, a limit of 92% of the ellipticity at 222 nm is recovered with essentially all of the biological activity recovered, similar to the results obtained when refolding from urea (Arakawa et al., 1985). Above pH 5.0, when heated, the molecule aggregates and precipitates, with the maximum rate of the aggregation and precipitation increasing dramatically between pH 5.0 and pH 6.0. Above pH 6.08 no further change in the rate of aggregation with increasing pH is observed. This series of observations indicates that HuIFN- $\gamma$  aggregates in both a temperature-dependent and a pH-dependent manner.

Figure 3 shows the corrected thermal denaturation profile for reversible unfolding at pH 6.0. Also shown are the relative aggregation rates at pH 6.0 taken from Table II and the mole fraction of the HuIFN- $\gamma$  available for binding to a monoclonal antibody. It can be seen that the aggregation correlates with the equilibrium concentration of the unfolded HuIFN- $\gamma$  and the mole fraction of HuIFN- $\gamma$  in solution.

Table II shows the effect of pH on  $T_m$ . Reversible equilibrium thermal unfolding profiles can be obtained from pH 4.75 to pH 6.25 if 0.25 M guanidine hydrochloride is included in the buffers. The  $T_m$  increases as the pH increased from 4.75 to 6.25.

Figure 4 shows the thermally induced aggregation kinetics of IFN- $\gamma$  from three species. Compared to HuIFN- $\gamma$ , neither the bovine nor the rabbit interferon  $\gamma$  form appreciable aggregates at pH 6.0 in the absence of GuHCl.

The role of histidine in this process is investigated by modifying the HuIFN- $\gamma$  molecule with two histidine-specific chemical modification reagents, ruthenium(III) pentaammine

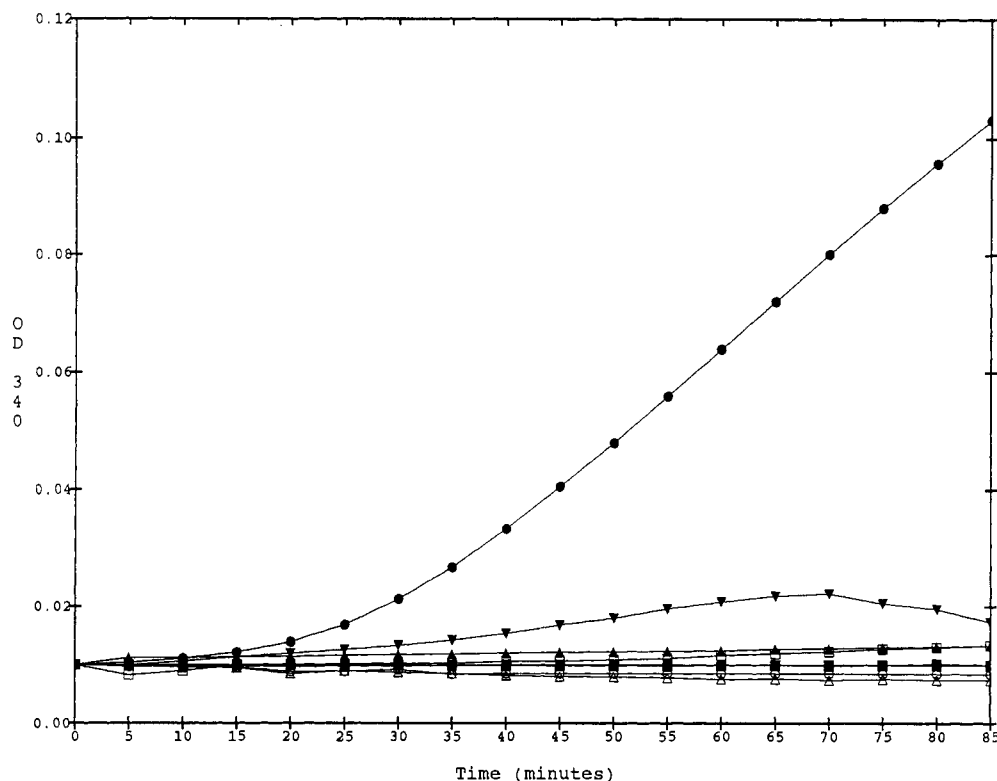


FIGURE 4: Comparison of the aggregation profiles of interferon  $\gamma$  derived from various species. Reactions at pH 5 are performed in 0.01 M acetic acid, pH 5. Reactions at pH 6 are performed in 0.01 M succinate, pH 6. The data show the increase in optical density at 340 nm of (●) HuIFN- $\gamma$  at pH 6, (○) HuIFN- $\gamma$  at pH 5.0, (▼)  $\text{Ru}^{3+}(\text{NH}_3)_5$ -HuIFN- $\gamma$  at pH 6.0, (▽)  $\text{Ru}^{3+}(\text{NH}_3)_5$ -HuIFN- $\gamma$  at pH 5.0, (△) BoIFN- $\gamma$  at pH 5.0, (▲) BoIFN- $\gamma$  at pH 6.0, (□) rabbit IFN- $\gamma$  at pH 5.0, and (■) rabbit IFN- $\gamma$  at pH 6.0. All reactions are performed at 50 °C.

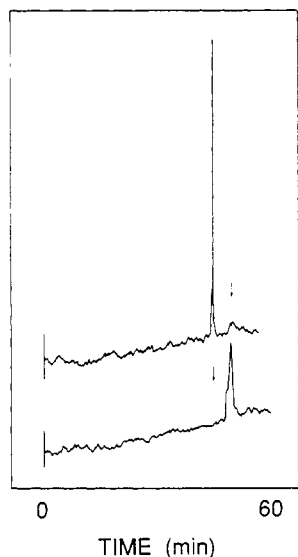


FIGURE 5: Preparation of  $\text{Ru}^{3+}(\text{NH}_3)_5$ -HuIFN- $\gamma$ . The top profile shows the elution position of HuIFN- $\gamma$ . The bottom profile shows the elution position of  $\text{Ru}^{3+}(\text{NH}_3)_5$ -HuIFN- $\gamma$ . The gradient is 10–60% acetonitrile.

(Sundberg & Gupta, 1972; Yocom et al., 1982) and ethoxyformic anhydride (Saluja & McFadden, 1980). Progress in the formation of  $\text{Ru}^{3+}(\text{NH}_3)_5$ -HuIFN- $\gamma$  is monitored by using HPLC. The HPLC profiles of HuIFN- $\gamma$  and  $\text{Ru}^{3+}(\text{NH}_3)_5$ -HuIFN- $\gamma$  are shown in Figure 5. The bottom HPLC profile shows the HuIFN- $\gamma$  is converted to at least the monoadduct.

Figure 4 shows this chemically modified molecule is stable to thermally induced aggregation at 50 °C at either pH 5.0 or pH 6.0. Figure 6 shows that this derivative is also stable at pH 6.0 and 65 °C compared to unreacted HuIFN- $\gamma$ .

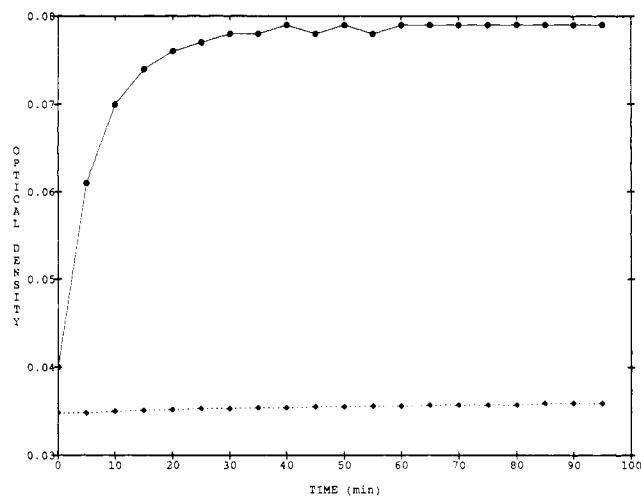


FIGURE 6: Aggregation of IFN- $\gamma$  and  $\text{Ru}^{3+}(\text{NH}_3)_5$ -rHuIFN- $\gamma$  at 65 °C. The buffer used is 0.01 M succinate at pH 6.0. (◆)  $\text{Ru}^{3+}(\text{NH}_3)_5$ -HuIFN- $\gamma$ ; (●) HuIFN- $\gamma$ .

In contrast to the ruthenium modification, reaction of HuIFN- $\gamma$  with ethoxyformic anhydride renders the molecule unstable, so much so that the product of this reaction aggregates at all temperatures from 5 to 25 °C. Analysis of the reaction products by HPLC (data not shown) indicates multiple species, but no thermal analysis was possible. Reactions of ethoxyformic anhydride with  $\text{Ru}^{3+}(\text{NH}_3)_5$ -HuIFN- $\gamma$  or with histidine-free BoIFN- $\gamma$  do not cause aggregation, again implicating the histidines in the reaction.

## DISCUSSION

Irreversible thermal denaturation of many proteins is thought to proceed via the preliminary unfolding of the native structure to an unfolded state that then readily aggregates

(Lumry & Biltonen, 1968). This can be formulated as the mechanism



in which N and U are collections of native and unfolded microstates in equilibrium and X is a collection of inactive molecules kinetically and/or thermodynamically blocked from returning to U. This mechanism suggests that the features stabilizing N to the reversible unfolding reaction will stabilize N to irreversible denaturation. This also suggests that the dependence of the kinetics of irreversible denaturation or aggregation on temperature will correlate well with the thermally induced reversible unfolding curve. The relationship between unfolding  $T_m$  and inactivation kinetics has been suggested by the temperature dependence of the inactivation of many proteins (Lumry & Biltonen, 1968; Zale & Klibanov, 1983). The mechanism does not account for all protein aggregation, however. For example, the folded states of some proteins are susceptible to aggregation. This is especially true in the case of pH-dependent aggregation, where proteins become more sensitive to aggregation as the solution pH approaches the *pI* of the protein.

In this study, we present data suggesting that HuIFN- $\gamma$  undergoes thermal irreversible denaturation by the aggregation of a thermally unfolded state. The dependence of the aggregation rate on temperature resembles the melting curve for the reversible unfolding of the molecule under similar conditions. It can be seen in Figure 3 that the aggregation rate at pH 6.0 correlates with the equilibrium concentration of unfolded HuIFN- $\gamma$  at the same pH as well as with the mole fraction of HuIFN- $\gamma$  which remains accessible to a monoclonal antibody after heating. The dependence of thermal inactivation on folding stability has also been observed in a thermally stable sequence variant of HuIFN- $\gamma$  (Mulkerrin and Wetzel, unpublished data).

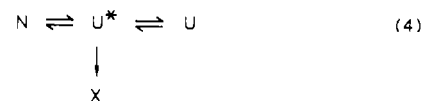
Additional support for the dependence of aggregation on unfolding is found in the correlation between the lag phase in the aggregation kinetics and the fast phase detected in the unfolding kinetics (Table I). The slow unfolding kinetics of HuIFN- $\gamma$  are somewhat unusual and will be discussed in a further treatment of the reversible unfolding to be published separately.

Table II shows the dependence of the thermodynamic stability of HuIFN- $\gamma$  on pH in the pH range 4.75–6.25. Within this range, the  $T_m$  increases from 30.5 to 40.5 °C as the pH increases from 4.5 to 5.5 and then changes relatively little from pH 5.5 to pH 6.25. Thus, it appears that decreasing the pH from 6.00 to 4.75 destabilizes the folded structure, in analogy to the behavior of other globular proteins. This effect is mediated by the unfavorable alteration of the electrostatic network of the molecule in a global, cooperative process (Brandts, 1968; Privalov, 1979).

While decreasing the pH from 6.0 to 5.0 destabilizes the molecule to reversible unfolding, this pH change stabilizes the molecule to thermal irreversible denaturation. Figure 2 shows the rate of thermally induced aggregation changes little from pH 8.5 to pH 6.0 but decreases to near zero at pH 5.0. Thus, while HuIFN- $\gamma$  at pH 6.0 follows the general mechanism for thermal aggregation shown in the above equation, this mechanism alone is not adequate to describe the effect of pH on thermal aggregation. Since the folded structure of HuIFN- $\gamma$  is destabilized at pH 5.0 compared to 6.0, stabilization toward aggregation at pH 5.0 must be due to some other consequence of protonation. Protonation might affect the solubility of an unfolding intermediate or of the final thermally unfolded state. Alternatively, protonation might increase the

rate of conversion of some poorly soluble unfolding intermediate. Recently, Brems et al. (1988) have demonstrated the role of an unfolding intermediate in the aggregation of bovine growth hormone.

The biphasic unfolding kinetics observed at pH 5.0 suggest the existence of at least one unfolding intermediate in the reversible unfolding pathway. Furthermore, the correlation of the lag time for aggregation with the kinetics of the fast phase of the reversible unfolding reaction suggests the involvement of a folding intermediate, and not the fully unfolded state, in the thermal aggregation. Some possible explanations for the effects of pH and chemical modification on thermal stability of HuIFN- $\gamma$  toward aggregation also require the existence of an unfolding intermediate. Thus, the mechanism



would better describe the reversible and irreversible thermal denaturation results, where  $U^*$  is an unfolding intermediate and U is the final unfolded state.

A striking feature of the aggregation rate vs pH profile is its resemblance to a titration curve, with the half-maximal rate at pH 5.7. Several residue types titrate near pH 5.7. Aspartate and glutamate have  $pK_a$ 's of about 4.5, histidine 6.5, and  $\alpha$ -amino groups about 7.8. Though pH 5.7 is lower than the average  $pK_a$  of histidine in proteins, it is within the observed range of pH 5.5–8.1 for histidines found in myoglobin (Matthew, 1985). In addition, a pH titration of HuIFN- $\gamma$  by NMR indicates that the two histidines in the molecule, H19 and H111, titrate in the range of pH 5–6 (M. G. Mulkerrin and P. D. Johnston, unpublished results).

Histidine protonation is further suggested in the pH dependence of aggregation by the behavior of two homologous IFN- $\gamma$  molecules obtained by the expression of the cloned genes in *E. coli*. BoIFN- $\gamma$  (68% homologous with HuIFN- $\gamma$ ) contains no histidine residues while rabbit interferon  $\gamma$  (63% homologous with HuIFN- $\gamma$ ) contains two histidines, but at positions 10 and 63 rather than at positions 19 and 111. Figure 4 shows that these interferons are considerably more stable to thermal inactivation at 50 °C than is HuIFN- $\gamma$ . This is not due to any increased  $T_m$  in these molecules, both of which are between 40 and 50 °C at pH 6.0 (unpublished observations).

To further explore the role of histidine protonation, we carried out selective chemical modification of histidine residues in HuIFN- $\gamma$ . As the data indicate, modification of at least one histidine in the molecule with ruthenium pentaamine stabilizes it to thermal aggregation at pH 6.0. One possible mechanism for this stabilization might be that the derivatization substantially increases the molecule's thermal stability so that it is folded at 50 °C. In fact, the ruthenium modification does increase the  $T_m$  of HuIFN- $\gamma$  (from 42 to 50 °C at pH 5.0) in an interesting parallel to its ability to increase the thermal stability of labeled DNA (Rubin et al., 1983). However, a repeat of the aggregation kinetics at pH 6.0 and at 65 °C, where the ruthenium derivative is fully unfolded, also shows no aggregation of the ruthenium-labeled HuIFN- $\gamma$ , compared to the rapid aggregation of the native molecule (Figure 6). Thus, the modification seems to change some property of a thermally unfolded state.

These results are consistent with the following interpretation. In the titration of HuIFN- $\gamma$  from pH 5 to pH 6, the change in the overall electrostatics of the molecule has the effect of increasing the thermodynamic stability of interferon, so that

more energy is required to unfold the molecule. In the same pH transition, however, the loss of positive charge, possibly via the deprotonation of one or both of the histidines, produces a dramatic change in the solubility properties of a thermally unfolded state, rendering it more susceptible to aggregation. In parallel, chemical modification which replaces the ionizable proton on one or both of the histidines with positive charge (+3) stabilizes the unfolded state throughout the pH range 5–6. In contrast, chemical modification with ethoxyformic anhydride, which replaces the ionizable histidine proton with a neutral group, produces a protein which aggregates readily even at 5 °C.

In the homologous animal interferons, these histidines are replaced with small hydrophilic residues: histidine-19 to threonine and histidine-111 to serine. If these histidine residues are involved in the observed aggregation, this suggests that interferons containing small charged or hydrophilic residues at these positions will be, in their thermally unfolded state, much less susceptible to aggregation than molecules with histidine at these positions. This hypothesis is now being tested in our lab using site-directed mutagenesis.

The effect of deprotonation to destabilize the thermally unfolded state may come about in a number of ways. In analogy to the relationship between *pI*, pH, and solubility found for the folded states of globular proteins, the solubility of an unfolded state of HuIFN- $\gamma$  may be decreased as the pH approaches its *pI*. At pH 6, however, even assuming all the Asp, Glu, and His residues of HuIFN- $\gamma$  are deprotonated, its net charge is still +8, quite far from the low net charge usually associated with decreased solubility. An interesting possibility is that deprotonated histidine plays a chemical role in the aggregation through complexation with metal ions in the buffer. If true, this would suggest a general mechanism by which proteins might denature irreversibly in the neutral pH range. However, aggregation kinetics of HuIFN- $\gamma$  at pH 6 and at 50 °C show no dependence on the presence or the absence of 10 mM EDTA in the buffer. A third possibility is that the aggregating species possesses some regular structure, as in an unfolding intermediate, for example, and that the protonation state of HuIFN- $\gamma$  either determines the extent to which it is populated in the melting transition or determines its solution properties when it is formed. We feel the results discussed here favor this interpretation. The suggestion of a functionally significant structure in the unfolded state of a protein has also been observed in work with analogues of T4 lysozyme, where the presence or absence of a disulfide bond alters the aggregation properties of the thermally unfolded protein (Wetzel et al., 1988, 1989).

#### ACKNOWLEDGMENTS

We thank Jeffrey Gorrell for providing us with HuIFN- $\gamma$ , Lewis E. Burton for providing us with BoIFN- $\gamma$  and rabbit IFN- $\gamma$ , and John R. Rubin for helpful discussions and suggestions. We gratefully acknowledge R. Baldwin and M. Laskowski for pointing out the possibility of metal ion complexation by histidine.

**Registry No.** Histidine, 71-00-1.

#### REFERENCES

- Arakawa, T., Alton, N. K., & Hsu, Y.-H. (1985) *J. Biol. Chem.* **260**, 14435.
- Arakawa, T., Hsu, Y.-H., & Yphantis, D. A. (1987) *Biochemistry* **26**, 5428.
- Brands, J. F. (1968) in *Structure and Stability of Biological Macromolecules* (Timasheff, S. N., & Fasman, G. D., Eds.) p 213, Marcell Decker, New York.
- Brems, D. N., Plaisted, S. M., Havel, H. A., & Tomich, C. C. (1988) *Proc. Natl. Acad. Sci. U.S.A.* **85**, 3367.
- Cancellieri, A., Frontali, C., & Gratton, E. (1974) *Biopolymers* **13**, 735.
- Chang, C. T., & Yang, J. T. (1977) *Anal. Lett.* **10**, 1195.
- Foon, T. E., Sherwin, S. E., Arams, P. G., Stephenson, H. C., Holmes, P., Mauish, A. E., Oldham, R. K., & Herberman, R. B. (1985) *Cancer Immunol. Immunother.* **20**, 193.
- Gray, P. W., Leung, D. W., Pennica, D., Yelverton, E., Najarian, R., Simonsen, C. C., Derynck, R., Sherwood, P. J., Wallace, D. M., Berger, S. L., Levinson, A. D., & Goeddel, D. V. (1982) *Nature* **295**, 503.
- Langer, J. A., & Pestka, S. (1985) *Pharmacol. Ther.* **27**, 371.
- Leach, S. J., & Scheraga, H. A. (1960) *J. Am. Chem. Soc.* **82**, 4790.
- Lumry, R., & Eyring, H. (1954) *J. Phys. Chem.* **58**, 110.
- Lumry, R., & Biltonen, R. (1968) in *Structure and Stability of Biological Macromolecules* (Timasheff, S. N., & Fasman, G. D., Eds.) pp 65–212, Marcell Decker, New York.
- Matthew, J. B. (1985) *Annu. Rev. Biophys. Biophys. Chem.* **14**, 382.
- Matthew, J. B., Gurd, F. R. N., Garcia Moreno, E. B., Flanagan, M. A., March, K. L., & Shire, S. J. (1985) *CRC Crit. Rev. Biochem.* **18**, 91.
- Matthews, C. R., Recchia, J., & Froebe, C. L. (1981) *Anal. Biochem.* **112**, 329.
- Mulkerrin, M. G., & Wetzel, R. (1987) *J. Interferon Res.* **7**, 751.
- Mulkerrin, M. G., Perry, L. J., & Wetzel, R. (1986) *UCLA Symp. Mol. Cell. Biol.* **32**, 297.
- Mutsaers, J. H. G. M., Kamerling, J. P., Devos, R., Guisez, Y., Fiers, W., & Vliegthart, J. F. G. (1986) *Eur. J. Biochem.* **156**, 651.
- Paulson, D. R., Addison, A. W., Dolphin, D., & James, B. R. (1979) *J. Biol. Chem.* **254**, 7002.
- Privalov, P. L. (1979) *Adv. Protein Chem.* **33**, 167.
- Rinderknecht, E., O'Connor, B. H., & Rodriguez, H. (1984) *J. Biol. Chem.* **259**, 5790.
- Rubin, J. R., Sabat, M., & Sundaralingam, M. (1983) in *Nucleic Acids; The Vectors of Life* (Pullman, B., & Jortner, J., Eds.) p 471, D. Reidel, Hingham, MA.
- Rubinstein, S., Familletti, P. C., & Pestka, S. (1981) *J. Virol.* **37**, 755.
- Saluja, A. K., & McFadden, B. A. (1980) *Biochem. Biophys. Res. Commun.* **94**, 1091.
- Sundberg, R. J., & Gupta, G. (1972) *Bioinorg. Chem.* **3**, 39.
- Tanford, C. J. (1964) *J. Am. Chem. Soc.* **86**, 2050.
- Tanford, C. J. (1968) *Adv. Protein Chem.* **23**, 121.
- Wetzel, R. (1988) *Protein Eng.* **2**, 1.
- Wetzel, R., Perry, L. J., Basse, W. A., & Bectel, W. J. (1988) *Proc. Natl. Acad. Sci. U.S.A.* **85**, 401.
- Wetzel, R., Perry, L. J., Mulkerrin, M. G., & Randall, M. (1990) in *Protein Design and the Development of New Therapeutics and Vaccines, Proceedings of the Sixth Annual Smith, Kline and French Research Symposium* (Poste, G., & Hook, G., Eds.) Plenum, New York (in press).
- Yocom, K. M., Shelton, J. B., Shelton, J. R., Schroeder, W. A., Worosila, G., Isied, S. S., Bordignon, E., & Gray, H. B. (1982) *Proc. Natl. Acad. Sci. U.S.A.* **79**, 7052.
- Yphantis, D. A., & Arakawa, T. (1987) *Biochemistry* **26**, 5422.
- Zale, S. E., & Klibanov, A. M. (1983) *Biotechnol. Bioeng.* **23**, 2221.
- Zoon, K. C., & Wetzel, R. (1984) *Handb. Exp. Pharmacol.* **71**, 79.